High Power 1.5μ m InGaAsP/InP Integrated Superluminescent Light Source

2001 Chinese Phys. Lett. 18 1074

(http://iopscience.iop.org/0256-307X/18/8/325)

High Power 1.5μm InGaAsP/InP Integrated Superluminescent Light Source *

LIU Yang(刘杨)[1], SONG Jun-Feng(宋俊峰)[1], ZENG Yu-Ping(曾毓萍)[1], WU Bin(吴宾)[1],
ZHANG Yuan-Tao(张源涛)[1], QIAN Ying(钱颖)[2], SUN Ying-Zhi(孙英志)[2], DU Guo-Tong(杜国同)[1]
[1]*Department of Electronic Engineering, State Key Laboratory on Integrated Optoelectronics, Jilin University, Changchun 130023*
[2]*Institute of Posts and Telecommunication, Jilin University, Changchun 130012*

(Received 24 December 2000)

The axis of the integrated superluminescent light source was tilted with respect to the output facet normal for lasing suppression. A new phenomenon (lasing suppression) was observed in the tilted integrated device. Three new schemes were proposed and demonstrated further to suppress the lasing by analysing the reason for lasing in the tilted structure. The lasing was suppressed successfully at high pumping levels, and high superluminescent powers (more than 300 mW) were obtained at a pulsed condition with the spectral full width at half maximum of 25–30 nm.

PACS: 42.50.Fx, 42.55.Px, 42.72.Ai, 42.82.−m

For future large-scale photonic networks, wavelength division multiplexing (WDM) systems are strongly desirable. Spectrum slicing[1−3] is one of the most attractive techniques for realizing multi-wavelength light sources in large-capacity dense WDM systems, in which a few narrowband lights can be filtered from a broadband light source. This technique is attractive because it can avoid the requirement for distributed feedback (DFB) laser arrays which have well-defined wavelengths. A superluminescent diode (SLD) is a good candidate for this broadband light source. However, the performance of the spectrum-sliced system has been severely limited by the available low output power of SLDs. To obtain high broadband optical power, researchers have proposed many tandem amplifying schemes.[4−8] In this letter, based on our original idea[8] about monolithic integration of the SLD with a semiconductor optical amplifier (SOA), the central axis of the device was tilted to the facet normal and a high amplified spontaneous emission (ASE) power at 1.5 μm was obtained by optimizing the tilted device structure.

The integrated superluminescent light source was fabricated on separate-confinement-heterostructure multiple-quantum-wells (SCH-MQWs) in a InGaAsP/InP wafer which was grown by metal–organic vapour phase epitaxy (MOVPE) on an InP substrate. The SCH active region consists of five compressively strained InGaAsP wells (7 nm thick) and tensilely strained InGaAsP barriers (10 nm thick). The integrated device possesses a gain-guide, oxide-stripe structure and it has two regions: the SLD region and the tapered SOA region (Fig. 1). The two regions can be pumped separately. The angle of the tapered SOA is 5°. To eliminate the facet reflection, the axis was tilted by 6° with respect to the normal to the facet. The typical device dimensions are as follows: the length of the SOA and SLD are 1500 and 300 μm, respectively; the stripe width of the SLD region is 3−5 μm; the width of the narrow and wide ends in the tapered SOA region are 3−5 μm and 130 μm, respectively. We do not adopt the scheme of anti-reflection (AR) coating to suppress the lasing because the radiative central wavelength varies along the wafer radius direction, which is due to the inhomogeneous layer thickness during epitaxy growth. Another reason is that ultra-low reflectivity is difficult to obtain at a wide wavelength range. Thus, this scheme is not suitable for mass production. The devices were mounted substrate-side down to the copper heat sink.

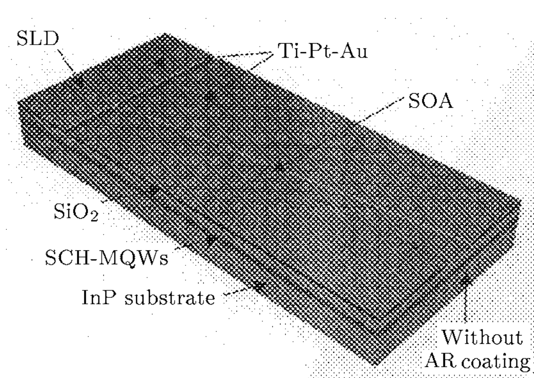

Fig. 1. Schematic diagram of the integrated superluminescent light source with tilted structure.

The performance of the integrated superluminescent devices was measured under a pulse condition (10 μs pulse width, 1% duty cycle). The superluminescent power (less than 80 mW) was obtained at a low pumping level. A higher power could not be

*Supported by "863" High Technology of China, the RFDP of China, "973" Key Fundamental Research Project of China (Grant No. G2000036605) and National Natural Science Foundation of China under Grant No. 60077021.

obtained because the lasing modes appeared with increasing current for the SOA. Encouragingly, a new phenomenon was discovered for the first time in which the lasing modes, to some extent, can be suppressed by injecting the current into the SLD region. This means that the tilted integrated devices possess the function of lasing suppression.

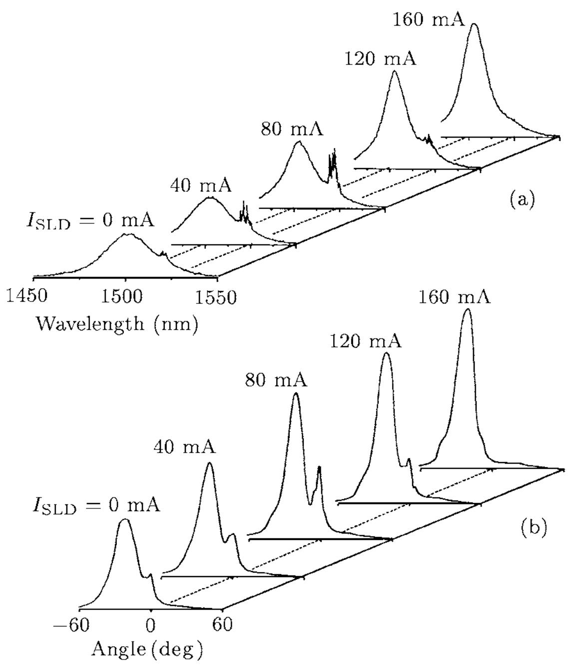

Fig. 2. Lasing suppression process, (a) spectrum and (b) far field pattern parallel to the junction plane, at different SLD currents when $I_{SOA} = 1.2$ A.

The entire process was investigated not only spectrally, as shown in Fig. 2(a), but also spatially. Figure 2(b) shows the corresponding far field patterns (FFPs) parallel to the junction plane. The main output beam was centred at about 20° to the facet normal, which is due to the tilted output axis. Another small peak which appeared at 0° was attributed to the laser lights, which was confirmed from the corresponding spectrum under the same pumping conditions. Moreover, we can also confirm (from the peak at 0°) that the lasing was attributed to the Fabry–Pérot (F–P) oscillations. Therefore, the peak at 0° in the FFP can be used as another criterion of lasing for the tilted devices.

We also detected the near field of the device. Figures 3(a)–3(c) show the infrared photographs of the near field in the cases before, during and after suppressing the lasing, respectively. Meanwhile, the corresponding position of the device is shown simultaneously in Fig. 3(d). It is evident that the route of lasing was located at line AB in Fig. 3(d), where the lasing gain length is maximum. This means that, although the light was attenuated in the un-pumped region, lasing can be established if the lasing gain length is long enough.

We consider that the process of lasing suppression is due to the competition of stimulated emission between the superluminescent photons that propagated along the tilted axis and the F–P oscillation photons. With the increasing incident light power from the SLD region, the incident photons gradually dominated the stimulated emission process and depleted the inverted carriers that previously participated in the lasing actions. As the gain of lasing modes decreases, the lasing is gradually suppressed. However, the lasing would not be suppressed if the SOA was pumped at a higher level because the high intensity of lasing photons have dominated the stimulated emission process. We think this is due to the easy lasing structure in the SOA region, in which the lasing gain length (shown in Fig. 1) was too long (900 μm and 50% of the total length of the device). This is easily understood from the J_{th} expression, which was obtained by imitating the threshold current condition of laser as follows,

$$J_{th} = J_0 + \frac{1}{lA}\left(\alpha L + \frac{1}{2}\ln\frac{1}{R_1 R_2}\right), \qquad (1)$$

where J_{th} is the lasing threshold current density of the integrated device, J_0 is the transparent current density, l is the maximum lasing gain length of the device (Fig. 3), L is the total length of the device, α is the absorption coefficient of the material, and R_1 and R_2 are the front and rear reflectivities of the cavity facet.

As is well known, lasing suppression is the key factor for a superluminescent device. Thus, in order to increase the ASE power, we should increase the lasing threshold current of the device. From this point of view, the decreasing l , R_1 or R_2 in Eq. (1) can all reach our target if the total length L of the device is fixed. Therefore, three schemes were proposed to further suppress lasing.

The first scheme is the so-called optimization of the angles of the tilted axis and the tapered SOA [Fig. 3(d)], in which the lasing gain length l can be reduced significantly. Considering the photon injection efficiency of SOA (because of emitting divergence from SLD) and the light output angle (governed by Snell's law), 3° and 7° were chosen for the taped and tilted angles, respectively. The calculated l is about 550 μm, only 30% of the total length if the length of the SLD and SOA are 300 and 1500 μm, respectively. The optimized devices have the same dimensions as those of the previous device, except for the different angles, and they were fabricated by using the same process mentioned above. Figure 4(a) simultaneously shows the spectrum and FFP for this optimized device, which indicated that no lasing mode appeared at a high pumping level. Figure 4(b) shows the typical $P - I$ curves of this device. It is evident that the integrated device presented the "soft" current threshold characteristics, which is the typical feature of the superluminescent device. Compared to the case when

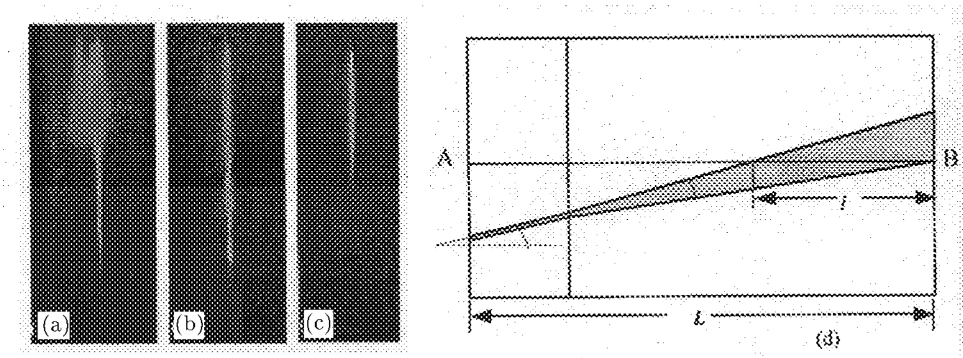

Fig. 3. Infrared near-field photographs of the near field in different cases: (a) before lasing, (b) during lasing and (c) after lasing suppression. (d) The corresponding position of the tilted device.

the SOA region only was pumped, the optical power increased notably because of the co-operation of the two regions, showing the superiority of the integrated device from the view of increasing optical power. High ASE power (220 mW) was obtained at 3.5 A for SOA and 400 mA for SLD, respectively.

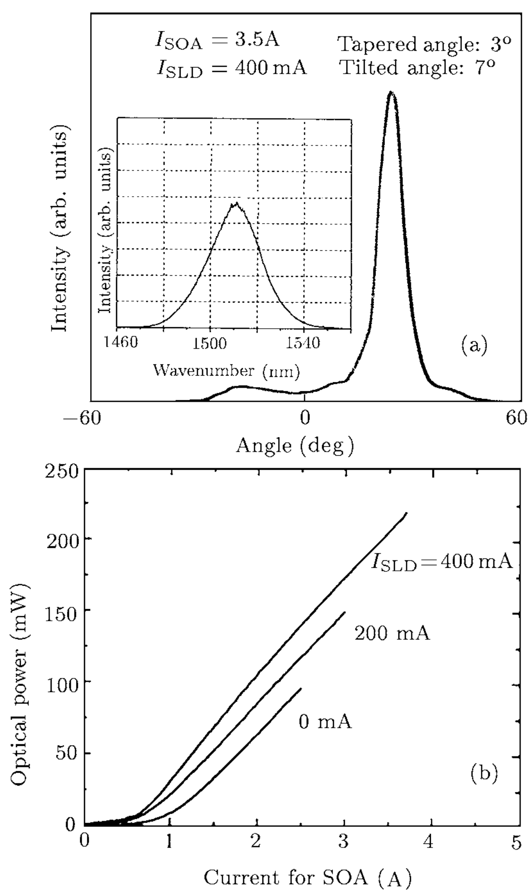

Fig. 4. (a) The far-field pattern and the corresponding spectrum (inset). (b) The ASE power versus current of SOA at different SLD current injection for the device with optimized angles (tapered angle 3° and tilted angle 7°).

The second scheme is that of adopting the ridge waveguide [Fig. 5(a)], in which the effective reflectivities (R_1 and R_2) can be significantly reduced. This is due to the fact that most lights will be guided along the titled axial direction if the ridge waveguide is adopted. The light that propagates along the vertical direction to the output cleaved facet will be deflected when they meet the edge of the ridge waveguide, because of the effective refractive index difference between the inside and outside regions of the ridge waveguide. Thus, the lights cannot reach the other cleaved facet perpendicularly, and so the lasing is destroyed. For a convenient comparison, we take the dimensions of this ridge waveguide device to be the same as those of the original device (tapered angle 5° and tilted angle 6°).

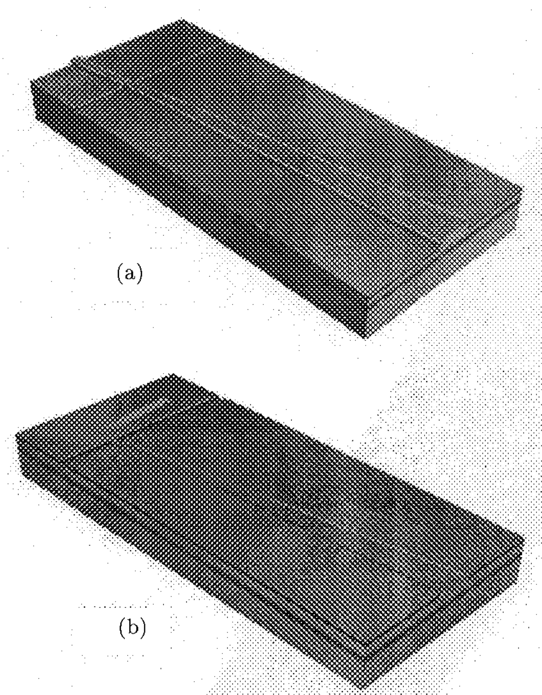

Fig. 5. Optimized integrated devices with (a) ridge waveguide and (b) deflecting slot.

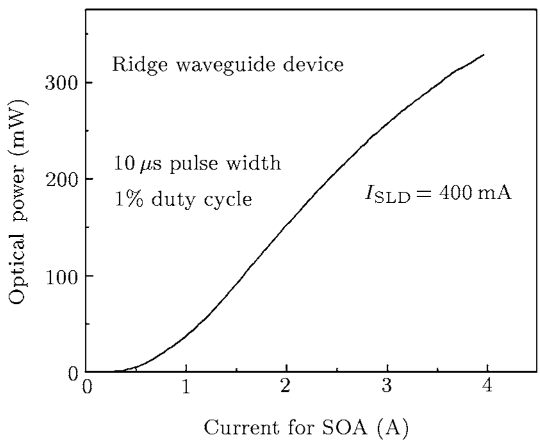

Fig. 6. Behaviour of $P - I$ for the device with the ridge waveguide.

The third scheme is that of etching a deflecting slot on the route of the optical oscillations [Fig. 5(b)]. The depth of the slot was 6 μm (etched through the active layer). The principle of this scheme is the same as that of the second scheme. The light reflected vertically from the output facet is scattered when meeting the deflecting slot and cannot reach the other facet, so the lasing cannot be established either.

Lasing has been suppressed successfully at high pumping level for all these three structure devices. Under the same pumping level, the highest ASE power was obtained from the ridge waveguide device, because of the less lateral current spreading in the ridge waveguide structure. More than 300 mW ASE power (Fig. 6) was achieved at 3.5 A for the SOA and 400 mA for the SLD, respectively. To our knowledge, this is the maximum ASE power that has been achieved at the same pumping level. The spectra of the three structure devices are similar, and the spectral full width at half maximum (FWHM) is 25−30 nm.

In conclusion, a high power 1.5 μm InGaAsP/InP integrated superluminescent light source with a tilted structure was fabricated, and a new phenomenon (lasing suppression) was discovered for the first time. Three new schemes were proposed and demonstrated to suppress lasing by analysing the reason for lasing in a tilted structure. The lasing was suppressed successfully at a high pumping level. A high superluminescent power (more than 300 mW) was obtained at a pulsed condition. The spectral FWHM was 25−30 nm.

References

[1] Jung D K, Shin S K, Lee C H and Chung Y C 1998 *IEEE Photon. Technol. Lett.* **10** 1334

[2] Liou K Y, Koren U and Dreyer K 1998 *IEEE Photon. Technol. Lett.* **10** 270

[3] Sampson D D and Holloway W T 1994 *Electron. Lett.* **30** 1611

[4] LEE J S and Chung Y C 1993 *IEEE Photon. Technol. Lett.* **5** 1458

[5] Kwong N S 1992 *IEEE Photon. Technol. Lett.* **4** 996

[6] Goldberg L and Mehuys D 1994 *Electron. Lett.* **30** 1628

[7] Liou K Y and Raybon G 1995 *IEEE Photon. Technol. Lett.* **7** 1025

[8] Du G T, Devane G, Stair K A, Wu S L, Chang R P H, Zhao Y S, Sun Z Z, Liu Y, Jiang X Y and Han W H 1998 *IEEE Photon. Technol. Lett.* **10** 57.